

Combined Bending and Axial Loading Responses of the Human Cervical Spine

James H. McElhaney, Brian J. Doherty, Jacqueline G. Paver,
and Barry S. Myers
Biomedical Engineering Dept.
Duke Univ.

Linda Gray
Dept. of Radiology
Duke University Medical Center

ABSTRACT

The lateral, anterior and posterior passive bending responses of the human cervical spine were investigated using unembalmed cervical spinal elements obtained from cadavers. Bending stiffness was measured in six modes ranging from tension-extension through compression-flexion. Viscoelastic responses studied included relaxation, cyclic conditioning and constant velocity deformation. A five-axis load cell was used to measure the applied forces. Results include moment-angle curves, relaxation moduli and the effect of cyclic conditioning on bending stiffness. The Hybrid III ATD neckform was also tested and its responses are compared with the human. It was observed that the Hybrid III neckform was more rate sensitive than the human, that mechanical conditioning changed the stiffness of the human specimens significantly, and that changing the end condition from pinned-pinned to fixed-pinned increased the stiffness by a large factor.

THIS PAPER DESCRIBES the results of a study of the bending responses of unembalmed human cervical spine segments. Considerable work has been done on the structural properties of the cervical spine and neck injury mechanisms. However, the cervical spine is an extremely complex structure, and many questions about its structural responses remain unanswered. Cervical injuries are of major interest because they occur with some frequency in automotive, recreational and sports activities, because they can involve the spinal cord with catastrophic and irreversible consequences, and because they usually involve the younger age groups. An extensive review of the literature was presented by Sances (1).

Many of the studies of the structural properties of the spine have involved compression. Perhaps the earliest such study was Messerer's work on the mechanical properties of the vertebrae (2). He reported compression breaking loads ranging from 1.47-2.16 kN for the lower cervical spine. Bauze and Ardran loaded human cadaveric cervical spines in compression and re-

ported forward dislocations with loads of 1.32-1.42 kN (3). However, their experiments were designed to force the dislocations to occur at a given vertebral level. Sances tested isolated cadaver cervical spines in compression, tension and shear (4). A quasi-static compression failure was observed at a load of 0.645 kN, and dynamic compression-flexion failures were reported at loads ranging from 1.78-4.45 kN. McElhaney *et al.* applied time-varying compressive loading to unembalmed human cervical spines (5,6). Failures were produced which are similar to those observed clinically with maximum loads ranging from 1.93-6.84 kN. In addition, it was found that small eccentricities in the load axis could change the buckling mode from posterior to anterior. Panjabi *et al.* measured rotation and translation of the upper vertebra as a function of transection of the components in single units of the cervical spine (7). Selecki and Williams conducted a study of cadaveric cervical spines loaded with a manually operated hydraulic jack (8). They were able to duplicate several types of clinically observed injuries, but reported loads in terms of the hydraulic pressure. Nusholtz *et al.* studied neck motions and failure mechanisms on unembalmed cadavers due to crown impacts; failure loads ranged from 3.2 to 10.8 kN (9). They reported that spinal response and damage were significantly influenced by the initial configuration of the spine.

Very few tests have been conducted on longer spinal segments. Edwards *et al.* tested lumbar spine motion units in combined loading (10). They found that stiffness of the motion unit was nonlinear and increased with increasing load. Markolf and Steidel tested human cadaveric thoracolumbar spine motion units in flexion, extension, lateral bending, torsion, and tension (11). They conducted free-vibration tests, and reported stiffness and damping values for the various test modes and vertebral levels. Panjabi *et al.* measured the three-dimensional stiffness matrix for all levels of the thoracic spine by measuring all components of deflection of spinal units for various loading modes (12). Roaf loaded single cervical spinal units in compression, extension, flexion, horizontal shear, and rotation (torsion) (13). He found that the intact disc,

lateral bending (TL). Two test configurations were utilized: (1) pinned-pinned end conditions (PP), and (2) fixed-pinned end conditions (FP).

For the pinned-pinned end conditions, the upper transfer bar was attached via a clevis to the load cell assembly, which was rigidly mounted to the upper platen of the MTS. The lower transfer bar was attached via a clevis to the ram of the MTS. The centerline of the specimen was parallel to, but not coincident with, the line of action of the MTS ram. The clevis end of the upper transfer bar was constrained from translation. The two external RVDTs were mounted on the test apparatus in order to measure the angular displacement of each transfer arm. In this configuration, the specimen was mounted with the superior end attached to the upper transfer bar and the inferior end attached to the lower transfer bar.

For the fixed-pinned end conditions, the upper clevis and corresponding RVDT were removed. In this configuration, the specimen was mounted with the superior end attached to the pivoting lower transfer bar and the inferior end fixed to the load cell assembly, which was rigidly mounted to the upper platen of the MTS.

A free body diagram of the test configuration is presented in Figure 2. The reference center line of the specimen is the central axis of the spinal foramen. The moment at the center of the specimen is

$$M_A = P_y a - P_z b,$$

and the moment measured by the load cell is

$$M_O = P_z B.$$

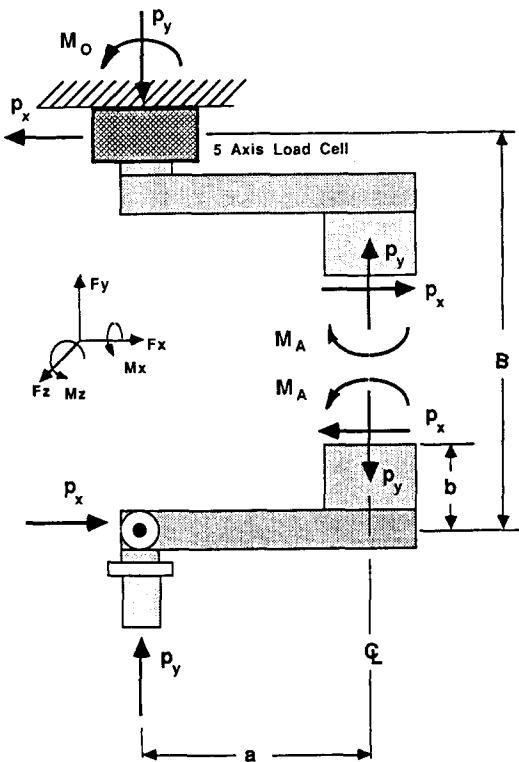


Figure 2: Freebody Diagram for the Fixed-Pinned Test Configuration

The moment induced by the shear force P_x was significant in the fixed-pinned configuration but was negligible in the pinned-pinned configuration. The apparatus had minimal overshoot and vibration below test frequencies of 5 Hz. Inertial forces begin to predominate above 10 Hz, and this is the current system's upper frequency range.

In this paper, test rates will be described in Hertz. The test period is the reciprocal of the frequency, and the time to peak load is one-half of the test period. The deformation rate is the maximum deformation in angular or linear units multiplied by twice the test frequency.

VISCOELASTIC TEST BATTERY - Five types of tests were performed in the following order:

1. Fully equilibrated relaxation test (the specimen was wet with isotonic saline for at least 24 hours pre-test.)
2. Cyclic test (nominally 40 cycles at 1.0 Hz until the waveform repeats.)
3. Mechanically stabilized or preconditioned relaxation test (the cyclic modulus reached an asymptotic plateau.)
4. Constant velocity tests (0.01 Hz, 0.1 Hz, 1.0 Hz, 5 Hz in the mechanically stabilized state.)
5. Constant velocity load to failure test (in the mechanically stabilized state.)

This battery of eight tests if performed in the six test modes results in forty-eight tests per specimen. If the end conditions were also varied (3 additional modes) there are one-hundred and forty-four combinations. Concern for specimen degradation resulted in approximately twenty-four tests per specimen actually being performed.

TEST RESULTS

RELAXATION TESTS - Pre-cyclic and post-cyclic relaxation tests were conducted to measure the viscoelastic responses of the spines in the initial equilibrated state and in the mechanically stabilized state. The relaxation tests were performed using ramp-and-hold command signals with 0.2 second rise times. The deflection was held constant for 125-150 seconds. Figure 3 is a typical example of the pre- (R1) and post-cyclic (R2) reduced (normalized by peak load) relaxation responses for spines in the equilibrated and mechanically stabilized states, respectively, tested in the pinned-pinned and fixed-pinned configuration. The response of the Hybrid III neck is shown for comparison.

The relaxation response of each spine reached a peak load for a finite loading rate, decreased monotonically, and approached asymptotically a non-zero equilibrium value during the test. A variable rate of moment relaxation was demonstrated. For constant deformations, the load decay was initially extremely rapid, decaying at a much slower rate thereafter. In all cases, the spines exhibited less load relaxation after cyclic preconditioning. The best least-squares fit, for all tests, of the reduced relaxation response was a linear regression in the natural log of time. This linear behavior in log time has also been observed for other biological tissues by Fung (18). These curves can be represented as a sum of exponentials, but this was not done since the exponents and amplitudes are quite sensitive to small changes in the data. Tables 2 and 3 show the mean and standard deviation (σ) of the instantaneous stiffness (K_0) and the asymptotic stiffness

TABLE 1. FAILURE TEST RESULTS.

SPECIMEN NUMBER	AGE/SEX	VERTEBRAL LEVELS	MAXIMUM MOMENT (N-m)	MAXIMUM AXIAL FORCE (N)	MAXIMUM A-P SHEAR (N)	ANGLE AT MAX. MOMENT (deg)	FAILURE CLASSIFICATION
1C P-P	52/M	C ₁ - T ₁	14.6	192	0	54	C ₄ -C ₅ , C ₅ -C ₆ ligamentum nuchae, ligamentum flavum, and post. long. ligament torn
2C P-P	64/F	C ₁ - T ₁	8.75	214	0	57	C ₆ -C ₇ ligamentum nuchae and R capsular ligament torn
3C P-P	N/A	C ₁ - T ₁	3.01	108	0	31	wedging of C ₄ -C ₅ bodies, C ₅ -C ₆ ligamentum nuchae disrupted
4C P-P	69/M	C ₁ - T ₁	3.40	338	11.7	40	wedging and broadening of C ₄ -C ₅ and C ₅ -C ₆ bodies, tear of C ₃ -C ₄ disc
5C P-F	77/M	C ₁ - T ₁					this specimen was not loaded to failure
6C P-F	76/M	BOS - T ₁	6.7	1513	23.0	15	C ₄ -C ₅ ant. disc disrupted, C ₂ -C ₃ , C ₃ -C ₄ , C ₄ -C ₅ L capsular ligaments partially disrupted
7C P-F	86/M	BOS - T ₁	10.2	2305	35	22	C ₄ -C ₅ , C ₅ -C ₆ , C ₆ -C ₇ shortened discs and wedged bodies, disrupted C ₇ -T ₁ disc, ligamentum nuchae and ligamentum flavum stretched

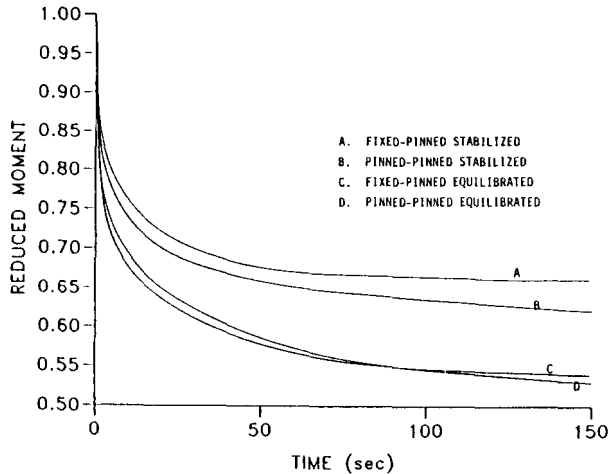


Figure 3: Typical Bending Moment Relaxation for Human Cervical Spines

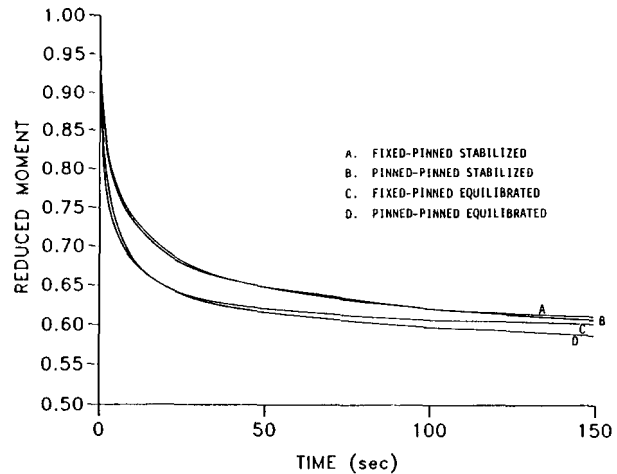


Figure 4: Typical Bending Moment Relaxation for the Hybrid III Neckform

(K_{∞}) for the various test modes of the human cervical spine and the Hybrid III neckform.

The ratio of K_0/K_{∞} is a measure of the time dependent or viscous component. For the fully equilibrated state the average value of K_0/K_{∞} for all tests was 1.838 for Hybrid III and 2.099 for the human cervical. For the mechanically stabilized state the average value was 1.658 for the Hybrid III and 1.507 for the human cervical. The ratio of the K_0 's for the equilibrated and the stabilized state is a measure of the nonlinear response probably due to the release of fluid from the various tissues. This ratio averaged for all tests was 1.623. For the Hybrid III, this ratio was very close to 1.

CYCLIC TESTS - Each fully equilibrated specimen was subjected to a sinusoidally varying displacement for approximately 50 cycles. The cyclic loading established the mechanically stabilized or preconditioned state (6). When a specimen was subjected to a repeated deformation history about a fixed length, the cyclic modulus magnitude decreased as the number of deformation cycles increased. In these tests, the cyclic modulus is the peak moment divided by the peak angular deformation (N-m/Radian). The initial cycle was representative of the response of the fully equilibrated spine. Eventually, after about 30 cycles, a steady-state (i.e. the mechanically stabilized state) was reached. The achievement of the mechanically stabilized state

Table 2. RELAXATION STIFFNESS (N-m/rad) FULLY EQUILIBRATED.

MODES	HUMAN												HYBRID III					
	FIXED-PINNED						PINNED-PINNED						FIXED-PINNED		PINNED-PINNED			
	K_0			K_∞			K_0			K_∞			K_0	K_∞	K_0	K_∞		
	Mean	σ	N	Mean	σ	N	Mean	σ	N	Mean	σ	N	Mean	σ	N	Mean	σ	N
CF	59.2	13.7	3	34.5	13.5	3							680.0	280.3	132.9	75.6		
TF	29.3		1	17.8		1	14.8		1	8.9		1	449.7	357.3	268.4	119.5		
CE							3.9	0.9	2	2.1	0.0	3	683.9	347.1	120.2	65.3		
TE							13.2		1	7.4		1	238.9	300.1	135.7	67.3		
CL	8.2	1.7	3	2.0	0.2	3	3.3	0.6	2	1.1	0.3	3	931.7	347.1	120.2	65.3		
TL	177.3		1	107.9		1	16.2		1	10.1		1	302.2	227.9	195.6	81.7		

TABLE 3. RELAXATION STIFFNESS (N-m/rad) MECHANICALLY STABILIZED.

MODES	HUMAN												HYBRID III					
	FIXED-PINNED						PINNED-PINNED						FIXED-PINNED		PINNED-PINNED			
	K_0			K_∞			K_0			K_∞			K_0	K_∞	K_0	K_∞		
	Mean	σ	N	Mean	σ	N	Mean	σ	N	Mean	σ	N	Mean	σ	N	Mean	σ	N
CF	36.9	6.9	3	31.8	4.7	3							656.5	282.4	134.0	87.4		
TF									10.5		1	7.0		1	524.2	349.0	157.2	89.2
CE							2.4	0.4	3	1.8	0.3	3	751.8	390.2	122.6	70.1		
TE	67.5		1	58.0		1	7.1		1	4.5		1	271.3	313.2	114.4	64.9		
CL	6.0	1.7	3	3.3	0.4	3	2.0	0.5	3	1.0	0.2	2	805.5	435.5	172.0	101.5		
TL							9.3		1	6.4		1	317.6	242.5	182.7	116.1		

σ = Standard Deviation; N = Number of Tests.

was evidenced by a constant cyclic modulus magnitude and a repeatable load-deflection response. Hopefully, after cyclic conditioning, the responses from one loading mode to another can be modeled using viscoelastic parameters which do not vary with time. The specimen could be returned to the fully equilibrated state by keeping it wet with isotonic saline in the refrigerator for 24 hours. Fung, who observed this phenomenon in other soft biological tissues, referred to this state as a preconditioned state (18). Figure 5 shows a typical family of moment conditioning cycles, while Table 3 provides the cyclic modulus for the various test modes. The instantaneous or fully equilibrated cyclic modulus K_0 (N-m/Radian) was computed as the ratio of the maximum moment and the bending angle. The mechanically stabilized or preconditioned cyclic modulus K_∞ was the above ratio after 40 cycles.

CONSTANT VELOCITY TESTS - Constant velocity tests were conducted on the mechanically stabilized spines using triangle wave deformations at frequencies of 0.01, 0.1, 1.0, 5 Hz, and, for some specimens, 10 Hz. The maximum ram displacement used for these test was the same as the maximum ram displacement used in the relaxation and cyclic tests. Thus, the deformation rate was varied by a factor of 500-1000.

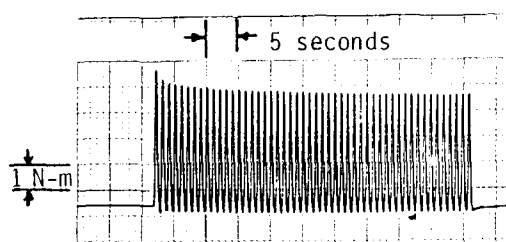


Figure 5: Typical Cyclic Test Envelope

Typical constant velocity moment-angle curves are presented for human and Hybrid III cervical spines in the pinned-pinned and fixed-pinned test configuration in Figures 6 and 7. All of the curves exhibit a hardening response (increasing stiffness) and hysteresis. The human and Hybrid III responses are fundamentally different. The Hybrid III shows the classic linear viscoelastic response of increasing stiffness with displacement rate while the human shows little change in stiffness or hysteresis over the rate range tested. Since these features of hysteresis, relaxation, and stiffness are not very sensitive to the rate of strain, simple linear viscoelastic models would not be appropriate pre-

TABLE 4. CYCLIC STIFFNESS (N-m/rad).

MODES	HUMAN 1st CYCLE						HUMAN 40th CYCLE						HYBRID III	
	FIXED-PINNED			PINNED-PINNED			FIXED-PINNED			PINNED-PINNED			FIXED-PINNED	PINNED-PINNED
	Mean	σ	N	Mean	σ	N	Mean	σ	N	Mean	σ	N	Mean	Mean
CF	206.3		1	4.9	1.4	3	105.0		1	4.3	0.9	3	567.3	153.2
TF	27.6		1	16.1		1	28.1		1	14.0		1	1216.4	185.2
CE	2.0		1	1.8		1	2.7		1	2.4		1	868.5	173.9
TE													710.1	137.5
CL	7.8	1.9	3	2.4	0.3	3	8.0	3.9	3	2.3	0.3	3	1054.2	209.5
TL	202.0		1	13.2		1	142.3		1	9.8		1	957.1	232.5

TABLE 5. CONSTANT VELOCITY STIFFNESS (N-m/rad).

MODES	HUMAN						HYBRID III	
	FIXED-PINNED			PINNED-PINNED			FIXED-PINNED	PINNED-PINNED
	Mean	σ	N	Mean	σ	N	Mean	Mean
CF	29.9	2.6	10	8.1	0.7	5	589.1	150.8
TF	41.8	5.6	5	14.8	1.3	5	608.4	199.0
CE				2.8	0.6	9	795.7	122.5
TE	309.0	26.9	5	10.3	1.2	11	232.1	138.8
CL	8.7	0.6	10	3.1	1.0	17	898.9	190.9
TL	254.1	34.6	5	13.0	1.9	5	442.0	226.1

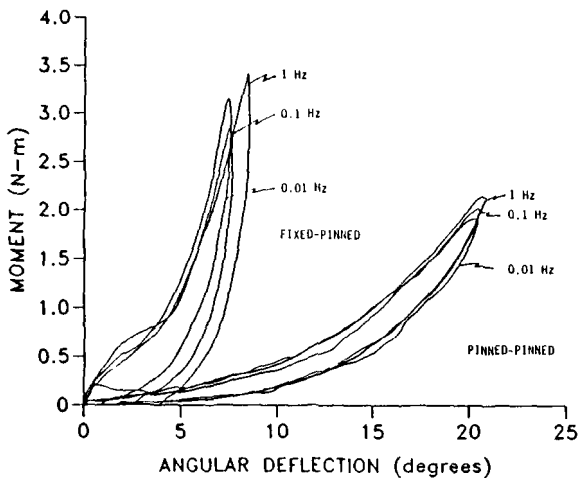


Figure 6: Typical Constant Velocity Profile for Human Cervical Spine

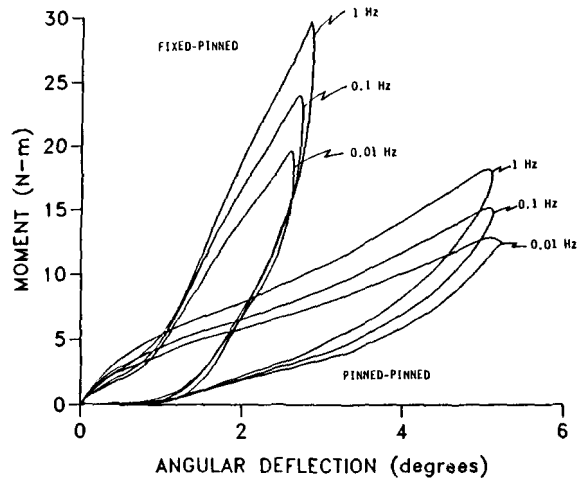


Figure 7: Typical Constant Velocity Profile for Hybrid III Neckform

dictors of the time dependent human spinal bending responses; and the more complex Maxwell-Weichert quasi-linear model is required (6).

Table 5 shows the stiffness averaged over four rates and all specimens. Three distinct tests of the Hybrid III were performed so that each value represents the mean of 12 tests. Several observations are apparent from this data. First, there are significant differences between the bending stiffnesses of the cadaver cervical spine and the Hybrid III. Second, there are significant differences in the bending stiffness of the cadaver cervical spine in the different modes. Tension-extension was the largest with a stiffness of 125 N-m/Radian, fixed-pinned and 15 N-m/Radian, pinned-pinned. Compression-lateral was the smallest with a stiffness of 10 N-m/Radian, fixed-pinned and 2.6 N-m/Radian pinned-pinned.

Figure 8 shows a typical response pattern for the human cervical spine to the various combined bending and axial loading modes. Figure 9 shows a typical response pattern for the Hybrid III.

FAILURE TESTS - After the battery of viscoelastic tests was accomplished, a constant velocity failure test at 0.1 Hz was performed. This rate was used so that fluoroscopic images of the specimen motion could be obtained. All failure tests were in the compression-flexion mode (CF). After the tests the specimens were examined with magnetic resonance imaging (MRI) and computerized tomographic radiography (CT), then dissected. Table 1 provides the maximum moment axial force and shear force applied to the specimen and the bending angle at which these peaks occurred. The first four tests (1C, 2C, 3C, 4C) were performed in the pinned-pinned mode and the remainder (6C, 7C) were tested in the fixed-pinned mode. In the pinned-pinned configuration the specimens were very flexible and were able to bend through on average of 45 degrees without an unstable dislocation. These specimens contained C_1 through T_1 and seven intact intervertebral structures. This is approximately 6.4 degrees per vertebral level. The shear forces were very small. The axial forces were low enough that the major stresses were due to the bending moment. The primary failure mechanism was disruption of the interspinous ligaments (ligamentum nuchae), the ligamentum flavum and capsular ligaments. There was also minor anterior wedging of the middle vertebral bodies and discs. In the pinned-pinned configuration the moment is maximum in the middle of the specimen. This may be the reason that the most frequent spinal cord injury level observed clinically is $C_4 - C_5$ and $C_5 - C_6$ (5).

In the fixed-pinned configuration much larger axial forces are required to produce the same bending moment because the shear force produces a counteracting moment. This is reflected in the failure mechanisms by superimposing compressively induced failures (wedging of bodies and discs) to the posterior tensile failures due to bending.

Figure 10 shows a composite of the moment-angle diagrams for the failure tests. The maximum moment ranged from 3.01 to 14.6 N-m. This large range is probably due to the variation in the size of the specimens. Specimen 1C and 7C had much larger vertebrae than the others as demonstrated by the CT scans.

DISCUSSION - This study demonstrated the complex, time-dependent responses of the human cervical spine and the Hybrid III neckform in combined axial and bending deformations. In all test

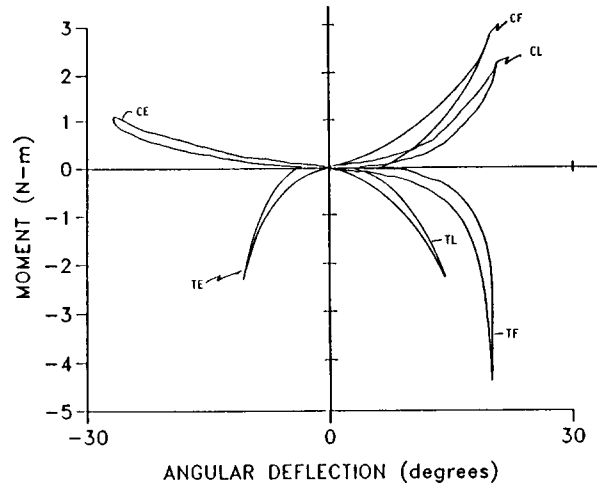


Figure 8: Typical Bending Responses of Human Cervical Spine

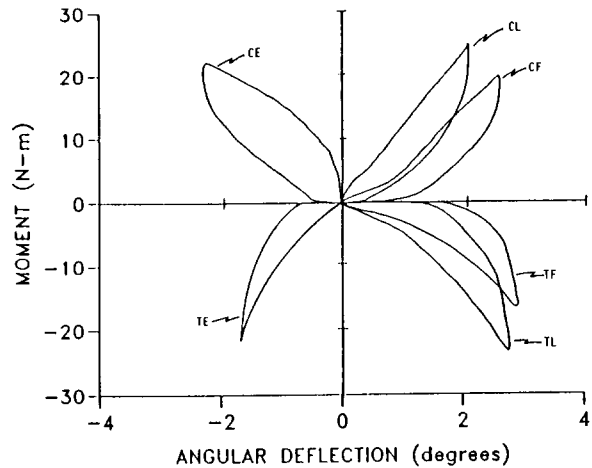


Figure 9: Typical Bending Responses of Hybrid III Neckform

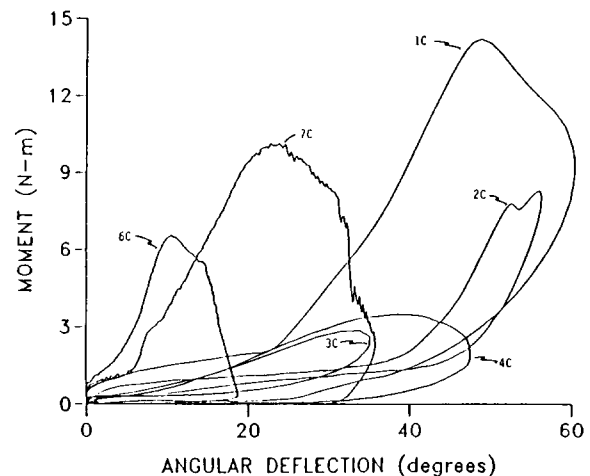


Figure 10: Failure Curves

modes (tension-extension, tension-flexion, tension-lateral bending, compression-extension, compression-flexion, compression-lateral bending) there was a large difference between the responses of spines in the fully equilibrated and mechanically stabilized states. In all test modes, the time-dependent responses included a significant viscoelastic exponential relaxation. The hysteresis and stiffness of the human specimens was only weakly dependent on strain rate.

There was a significant difference between the stiffness of the cadaver cervical spines and the Hybrid III. This was expected since the performance requirements of the Hybrid III were based on human volunteer data, and it is considered to represent a tensed human neck while the cadaver spines have no musculature present (19). The Hybrid III responses were the typical linear viscoelastic type. That is, a linear differential equation would provide an adequate model. The behavior of the human cervical spine was more complex, however, and requires a quasi-linear model (6).

The bending stiffness of the cervical spine was significantly influenced by the direction of the bending moment, the types of end restraint, the magnitude of the deformation, and the previous deformation history. After approximately thirty deformation cycles a mechanically stabilized state was attained that provided repeatable load-deformation responses. The tensile modes were consistently stiffer than the compressive modes. This may be due to a shift in the neutral axis toward the tensile side which pre-tensions slack ligaments and reduces the eccentricity.

Simple beam theory predicts doubling of the bending stiffness when comparing pinned-pinned and fixed-pinned ends. These tests showed an increase in stiffness of approximately eight times. The test apparatus used in these tests (and by most other researchers) constrained the pinned end to move in a straight line. This produced a shearing force which, acting over a relatively long moment arm, stiffened the specimen. This shearing force not only changes the moment acting on the specimen but also influences the failure mode. Several researchers have tested cervical specimens without well controlled and monitored end conditions. Most other works report only the axial load. These experiments indicate that when the loading is eccentric (as it almost always is), the primary deformation mode is bending; and the moment applied to the specimen is strongly influenced by shear forces and the magnitude of the eccentricity. The axial load is therefore a poor indicator of the type and magnitude of failure stresses.

ACKNOWLEDGEMENTS

This work was supported by the Department of Health and Human Services, Center for Disease Control grant R49/CCR402396-02, and by the Whitaker Foundation.

BIBLIOGRAPHY

1. Sances, A, Weber, R.C., Larson, S.J., Cusick, J.S., Myklebust, J.B., and Wash, P.R., "Bioengineering Analysis of Head and Spine Injuries," *CRC Critical Reviews in Bioengineering*, February, 1981.
2. Messerer, O., *Über Elasticität und Festigkeit der Menschlichen Knochen*, J. G. Cottaschen Buchhandlung, Stuttgart, 1880.
3. Bauze, R.J. and Ardran, M.J., "Experimental Production of Forward Dislocation in the Human Cervical Spine". *Journal of Bone and Joint Surgery*, 60B(2):239, 1978.
4. Sances Jr., A., Myklebust, J., Houterman, C., Webber, R., Lepkowski, J., Cusick, J., Larson, S., Ewing, C., Thomas, D., Weiss, M., Berger, M., Jessop, M.E., Saltzberg, B., "Head and Spine Injuries." *AGARD Conference Proceedings on Impact Injury Caused by Linear Acceleration — Mechanism, Prevention, and Cost*, 1982.
5. McElhaney, J.H., Roberts, V.L., Paver, J.G. and Maxwell, G.M., "Etiology of Trauma to the Cervical Spine," in *Impact Injury to the Head and Spine*, C.C. Thomas, 1982.
6. McElhaney, J.H., Paver, J.G., McCrackin, H.J., and Maxwell, G.M., "Cervical Spine Compression Responses," SAE Paper No. 831615, 1983.
7. Panjabi, M.M., White, A.A., and Johnson, R.M., "Cervical Spine Mechanics as a Function of Transection of Components," *Journal of Biomechanics*, 8(5):327, 1975.
8. Selecki, B.R., and Williams, H.B.L., "Injuries to the Cervical Spine and Cord in Man," Australian Med. Assoc., Mervyn Archdall Med. Monograph #7, Australian Medical Publishers, South Wales, 1970.
9. Nusholtz, G.S., Melvin, J.W., Huelke, D.F., Alem, N.M., and Blank, J.G., "Response of the Cervical Spine to Superior-Inferior Head Impact," *Proc. of the 25th Stapp Car Crash Conference*, SAE Paper No. 811005, pp. 197-237, 1981.
10. Edwards, W.T., Hayes, W.C., Posner, I., White, A.A. III, and Mann, R.W., "Variation of Lumbar Spine Stiffness With Load," *Journal of Biomechanical Engineering*, 109:35, 1987.
11. Markolf, K.L., and Steidel, R.S., Jr., "The Dynamic Characteristics of the Human Intervertebral Joint," ASME Paper No. 70-WA/BHF-6, 1970.
12. Panjabi, M.M., Brand, R.A., Jr., and White, A.A., "Three Dimensional Flexibility and Stiffness Properties of the Human Thoracic Spine," *Journal of Biomechanics*, 9:185, 1976.
13. Roaf, R., "A Study of the Mechanics of Spinal Injury," *Journal of Bone and Joint Surgery*, 42B:810, 1960.
14. Tencer, A.F., Ahmed, A.M., and Burke, D.L., "The Role of Secondary Variables in the Measurement of the Mechanical Properties of the Lumbar Intervertebral Joint," *Journal of Biomechanical Engineering*, 103:129, 1981.
15. Hodgson, V.R., and Thomas, L.M., "The Biomechanics of Neck Injury From Direct Impact to the Head and Neck," Head and Neck Injury Criteria, U.S. Government Printing Office, 1981.
16. Seemann, M.R., Muzzy, W.H. and Lustick, L.S., "Comparison of Human and Hybrid III Head and Neck Response," *Proc. of the Thirtieth Stapp Car Crash Conference*, 1986.
17. Hirsch, C., "Method of Stabilizing Autopsy Specimens in Biomechanical Experiments," *Acta Orthopaedica Scandinavia*, 34(4):374, 1964.
18. Fung, Y.C., "Stress-Strain History Relations of Soft Tissue in Simple Elongations," *Biomechanics — Its Foundation and Objectives*, Prentice-Hall, Inc., Englewood Cliffs, 1972.
19. Mertz, H.J., Neathery, R.F., and Culver, C.C., "Performance Requirements and Characteristics of Mechanical Necks, in *Human Impact Response*, Plenum Press, 1973.